Orthologous genes *Pm12* and *Pm21* from two wild relatives of wheat show evolutionary conservation but divergent powdery mildew resistance

Shanying Zhu[1,2,8], Cheng Liu[3,8], Shuangjun Gong[4,8], Zhaozhao Chen[2], Rong Chen[5], Tianlei Liu[2], Renkang Liu[2], Haonan Du[2], Rui Guo[2], Genying Li[3], Miaomiao Li[6], Renchun Fan[6], Zhiyong Liu[6], Qian-Hua Shen[6], Anli Gao[5,*], Pengtao Ma[7,*] and Huagang He[2,*]

[1]School of Environment and Safety Engineering, Jiangsu University, Zhenjiang 212013, China

[2]School of Life Sciences, Jiangsu University, Zhenjiang 212013, China

[3]Crop Research Institution, Shandong Academy of Agricultural Sciences, Jinan 250100, China

[4]Institute of Plant Protection and Soil Science, Hubei Academy of Agricultural Sciences, Wuhan 430064, China

[5]School of Life Sciences, Henan University, Kaifeng 475004, China

[6]State Key Laboratory of Plant Cell and Chromosome Engineering, Institute of Genetics and Developmental Biology, The Innovative Academy of Seed Design, Chinese Academy of Sciences, Beijing 100101, China

[7]College of Life Sciences, Yantai University, Yantai 264005, China

[8]These authors contributed equally to this article.

*Correspondence: Anli Gao (algao@henu.edu.cn), Pengtao Ma (ptma@ytu.edu.cn), Huagang He (hghe@ujs.edu.cn)

https://doi.org/10.1016/j.xplc.2022.100472

ABSTRACT

Wheat powdery mildew, caused by *Blumeria graminis* f. sp. *tritici* (*Bgt*), is a devastating disease that threatens wheat production worldwide. *Pm12*, which originated from *Aegilops speltoides*, a wild relative of wheat, confers strong resistance to powdery mildew and therefore has potential use in wheat breeding. Using susceptible mutants induced by gamma irradiation, we physically mapped and isolated *Pm12* and showed it to be orthologous to *Pm21* from *Dasypyrum villosum*, also a wild relative of wheat. The resistance function of *Pm12* was validated via ethyl methanesulfonate mutagenesis, virus-induced gene silencing, and stable genetic transformation. Evolutionary analysis indicates that the *Pm12/Pm21* loci in wheat species are relatively conserved but dynamic. Here, we demonstrated that the two orthologous genes, *Pm12* and *Pm21*, possess differential resistance against the same set of *Bgt* isolates. Overexpression of the coiled-coil domains of both PM12 and PM21 induces cell death in *Nicotiana benthamiana* leaves. However, their full-length forms display different cell death-inducing activities caused by their distinct intramolecular interactions. Cloning of *Pm12* will facilitate its application in wheat breeding programs. This study also gives new insight into two orthologous resistance genes, *Pm12* and *Pm21*, which show different race specificities and intramolecular interaction patterns.

Key words: *Pm12*, *Pm21*, powdery mildew resistance, evolutionary conservation, race specificity, intramolecular interaction

Zhu S., Liu C., Gong S., Chen Z., Chen R., Liu T., Liu R., Du H., Guo R., Li G., Li M., Fan R., Liu Z., Shen Q.-H., Gao A., Ma P., and He H. (2023). Orthologous genes *Pm12* and *Pm21* from two wild relatives of wheat show evolutionary conservation but divergent powdery mildew resistance. Plant Comm. **4**, 100472.

INTRODUCTION

Wheat powdery mildew, caused by the obligate biotrophic fungal pathogen *Blumeria graminis* f. sp. *tritici* (*Bgt*), is a devastating disease that threatens wheat production and yield worldwide. Incorporation of powdery mildew resistance (*Pm*) genes into susceptible wheat cultivars is the most effective, economical, and environmentally friendly means for controlling this disease. Tradi-

tional breeding methods take many years to introduce resistance, whereas cloned resistance genes could be transferred directly through a transgenic approach. Currently, more than 100 *Pm*

---

genes/alleles have been identified from common wheat and its cultivated or wild relatives (McIntosh et al., 2017; He et al., 2021a; 2021b). Only a few of these *Pm* genes have been cloned, such as *Pm1–Pm5* (Yahiaoui et al., 2004; Sánchez-Martín et al., 2016, 2021; Xie et al., 2020; Hewitt et al., 2021), *Pm8* (Hurni et al., 2013), *Pm17* (Singh et al., 2018), *Pm21* (He et al., 2018), *Pm24* (Lu et al., 2020), *Pm38/Yr18/Lr34/Sr57* (Krattinger et al., 2009), *Pm41* (Li et al. 2020), *Pm46/Yr46/Lr67/Sr55* (Moore et al. 2015), *Pm60* (Zou et al., 2018), and *WTK4* (Gaurav et al., 2022). *Pm3*, *Pm5*, *Pm21*, *Pm24*, *Pm38/Yr18/Lr34/Sr57*, *Pm41*, *Pm46/Yr46/Lr67/Sr55*, and *Pm60* were cloned by a map-based strategy. *Pm1*, *Pm2*, and *Pm4* were isolated based on a mutant sequencing strategy. *WTK4* was identified by genome-wide association study (GWAS). *Pm8* and *Pm17* were both isolated using a homology-guided approach based on the previously cloned *Pm3*.

The powdery mildew resistance gene *Pm21*, which originates from *Dasypyrum villosum* (2n = 2x = 14, VV), a wild diploid relative of wheat, confers immunity to all tested *Bgt* isolates and has been widely utilized in wheat breeding (Chen et al., 2013). However, it is difficult to clone *Pm21* on 6VS of *D. villosum* owing to the restriction of exchange between the alien and wheat homoeologous chromosomal arms (Qi et al., 1998). Using the gene chip technique, Cao et al. (2011) identified a candidate gene, *Stpk-V*, from the *Pm21* region, which encoded a serine-threonine kinase that enhanced powdery mildew resistance when overexpressed in common wheat. He et al. (2017) identified susceptible *D. villosum* accessions from a natural population and performed fine genetic analysis of *Pm21* using a mapping population derived from a cross between resistant and susceptible *D. villosum* accessions. Two nucleotide-binding and oligomerization domain (NOD)-like receptor (NLR) genes, but not *Stpk-V*, were located in the *Pm21* locus. Further functional analysis revealed that *DvRGA2*, one of the two NLR genes, is *Pm21* (He et al., 2018). Another study also verified the same NLR gene as *Pm21* via RenSeq-PacBio (Xing et al., 2018).

Pm12 also confers highly effective resistance to powdery mildew, as reported by several researchers (Niewoehner and Leath 1998; An et al., 2019; Zhang et al., 2019; Wan et al., 2021). *Pm12* was originally transferred from *Aegilops speltoides* (2n = 2x = 14, SS) into wheat cv. Wembley, generating Line #31 (Wembley Line #31, WL31). WL31 harbors the translocated chromosome 6BS-6SS.6SL (Miller et al., 1988; Jia et al., 1996). Subsequently, the introgression line 1338-8, which contains only a partial short arm of chromosome 6S (6SS), was generated from WL31. However, linkage drag, including delayed maturation and yield depression, could not be eliminated because of severe recombination suppression between chromosomes 6SS and 6BS (Song et al., 2007). Therefore, the powdery mildew resistance conferred by *Pm12* has rarely been used in breeding. Recombination suppression also greatly impeded the isolation of *Pm12* using traditional map-based cloning in a wheat background.

As an alternative to genetic analysis, chromosomal deletion analysis is also an efficient method for finely mapping a gene of interest (Zhu et al., 2018). Here, using chromosome deletion lines induced by irradiation that are susceptible to powdery mildew,

we quickly revealed that the *Pm12* locus corresponds to the *Pm21* orthologous region of *Ae. speltoides* based on molecular marker analysis combined with comparative genomics analysis. We now report the isolation and functional validation of *Pm12* via ethyl methanesulfonate (EMS)-induced mutagenesis, virus-induced gene silencing (VIGS), and stable wheat transformation. We demonstrate a significant difference between the two orthologous genes *Pm12* and *Pm21* through comparative analyses of their resistance spectra and intramolecular interaction patterns. We also reveal the evolutionary dynamics of orthologous *Pm12*/*Pm21* loci in Triticeae species.

RESULTS

Chromosomal deletion analysis suggests that *Pm12* might be orthologous to *Pm21*

Ae. speltoides Pm12 (6SS) and *D. villosum Pm21* (6VS) are both located on the short arms of the homoeologous group 6 chromosomes. To evaluate the collinearity relationship, we used a set of *Pm21*-associated 6VS markers reported previously (He et al., 2016; Zhu et al., 2018) to detect the *Pm12* and *Pm21* regions. The results revealed that 9 of 46 6VS markers showed polymorphisms between *Pm12*-carrying materials (WL31 and 1338-8) and *Pm12*-null common wheat YM9. Another four polymorphic markers (*6SS-03*, *6SS-04*, *6SS-05*, and *6SS-07*) were newly developed in this study. Among the 13 polymorphic markers, 10 could simultaneously distinguish the alien chromosomes 6SS and 6VS in a wheat background (Supplemental Figure 1, Supplemental Table 1).

Seeds of line 1338-8 carrying *Pm12* were treated with ^{60}Co-γ-ray irradiation. From the 316 M_2 families, four susceptible mutants (1338-8-S1 to 1338-8-S4) were obtained (Figure 1A). The 13 6SS-specific markers described above were then used to detect whether there were alien chromosomal deletions in the four susceptible mutants. The result showed that the mutant lines 1338-8-S2 and 1338-8-S3 contained alien chromosomal deletions flanked by markers *6SS-03* and *6SS-05*, and *6SS-03* and *6SS-06*, respectively (Figure 1B). Thus, the *Pm12* locus could be narrowed to a relatively small physical region flanked by markers *6SS-03* and *6SS-05*, corresponding to *TraesCS6B02G146300* and *TraesCS6B02G151600*, respectively, in the B subgenome of the Chinese Spring reference genome, RefSeq v1.1 (International Wheat Genome Sequencing Consortium et al., 2018). Because most disease resistance genes belong to the NLR family, we checked the Chinese Spring genome sequence spanning *TraesCS6B02G146300* to *TraesCS6B02G151600* and found only one annotated NLR gene, *TraesCS6B02G148400* (Figure 1B). BLAST analysis showed that this gene was highly homologous to the recently cloned powdery mildew resistance gene *Pm21* from *D. villosum* (88% nucleotide identity; E value = 0). Further analysis showed that *TraesCS6B02G148400* fused two NLR genes corresponding to the two adjacent genes *DvRGA1* and *DvRGA2* (*Pm21*). In the recently published genome of *Ae. speltoides* accession AEG-9674-1 (Avni et al., 2022), a gene (*AE.SPELTOIDES.r1.6BG0531060*) highly homologous to *Pm21* was also found (94% identity; E value = 0). Molecular detection showed that marker *6SS-04* corresponding to *AE.SPELTOIDES.r1.6BG0531060* had no product in the susceptible mutants 1338-8-S2 and 1338-8-S3. Therefore,
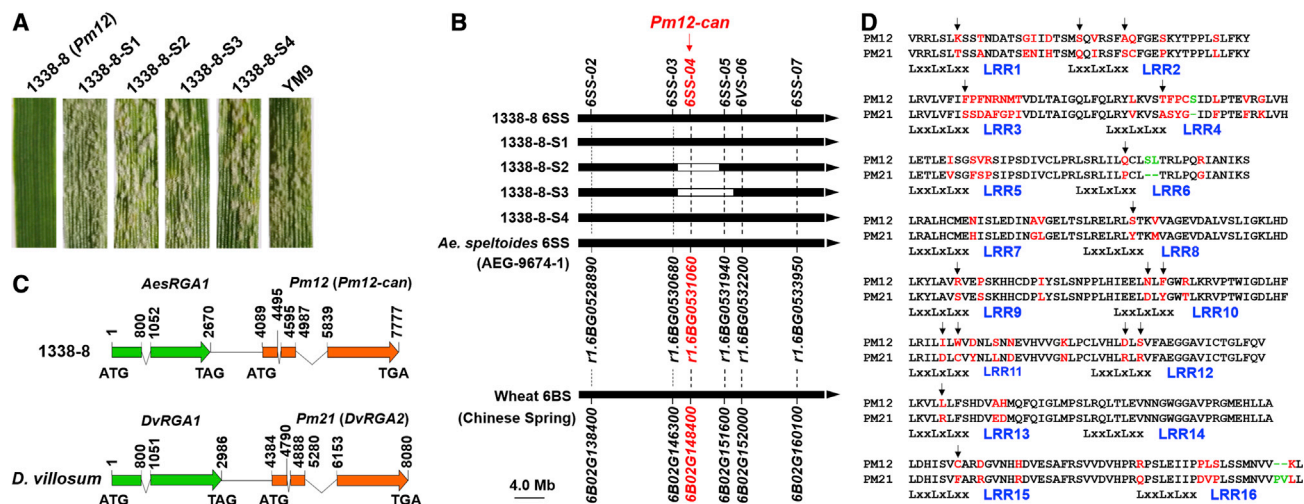
Figure 1. Physical mapping of *Pm12* and characteristics of the candidate gene *Pm12-can*.

(A) Powdery mildew-susceptible mutants obtained after ^{60}Co-γ-ray irradiation.

(B) Physical mapping of *Pm12* using chromosomal deletion mutant lines and comparative mapping using the reference genomes of *Ae. speltoides* accession AEG-9674-1 and wheat cv. Chinese Spring.

(C) Gene structures of *Pm12* and *Pm21*. Genes in the *Pm12* and *Pm21* loci are indicated by arrows that are broken by introns.

(D) Sequence comparison of the LRR domains encoded by *Pm12* and *Pm21*. Both LRR domains of PM12 and PM21 are divided into 16 LRR motifs (LRR1 to LRR16). LxxLxLxx motifs are marked below the corresponding sequences. L represents a leucine or another aliphatic amino acid residue, and x represents the predicted solvent-exposed LRR residue. Green amino acids or – indicate insertions/deletions, and red amino acids differ between PM12 and PM21. Arrows represent solvent-exposed LRR residues.

AE.SPELTOIDES.r1.6BG0531060, the ortholog of *Pm21*, was considered to be a candidate for *Pm12*. In lines 1338-8-S1 and 1338-8-S4, the specific bands of marker *6SS-04* were present. We suggest that the candidate gene may contain minor change(s) that require further analysis.

The *Pm12* candidate, *Pm12-can*, shares high identity and the same exon–intron structure with *Pm21*

In the *Pm21* locus, two NLR genes, *DvRGA1* and *DvRGA2* (*Pm21*), with typical coiled-coil (CC), nucleotide-binding site (NBS), and leucine-rich repeat (LRR) domains are paralogous and closely linked. According to their conserved sequences, we designed three primer pairs to isolate *Pm12*-related DNA fragments from the genomic DNA of line WL31. The downstream sequence of the candidate gene was obtained using the TAIL–PCR method (Supplemental Figure 2). Finally, a 9355-bp genomic sequence from WL31 was assembled. This sequence contained two NLR genes, *AesRGA1* (*DvRGA1-like* gene) and *Pm12-can* (the candidate for *Pm12*, *DvRGA2-like* gene). The *Pm12-can* sequence was identical to that in the recently published genome of *Ae. speltoides* accession AEG-9674-1 (Avni et al., 2022) and differed in only one base from the genome sequence of *Ae. speltoides* accession TS01 (Li et al., 2022), leading to the amino acid change R769Q. We concluded that the sequence we obtained originated from *Ae. speltoides* chromatin introgressed into wheat. Through comparing sequences of the above genomic DNA and its corresponding cDNA obtained by RT–PCR, we found that *Pm12-can* and *Pm21* have the same gene structure, consisting of three exons and two introns (Figure 1C). The transcription of both *Pm-can* and *Pm21* was slightly activated when challenged with Bgt01 (Supplemental Figure 3).

The coding sequence of *Pm12-can* shares 89.9% and 72.8% identity with those of *Pm21* and its paralog *DvRGA1*, respectively. In addition to five InDels, there were 268 SNPs, including 133 synonymous SNPs and 135 non-synonymous SNPs, between *Pm12* and *Pm21* (Supplemental Table 2). Sixty-three of 135 amino acid changes appeared in the LRR domain, 16 of which were located in the solvent-exposed LRR residues (Figure 1D) that may alter recognition specificity to the powdery mildew pathogen (Wulff et al., 2009). The putative protein of *Pm12-can* showed the highest identity with PM21 (84.9%), relatively lower identity with DvRGA1 (64.2%), and low identities with the powdery mildew resistance proteins PM1a, PM2, PM3b, PM5e, PM8, PM17, PM41, and PM60 and other disease resistance proteins (<36%).

Pm12-can is necessary for resistance, as shown by mutational and VIGS analyses

To further examine whether *Pm12-can* is responsible for disease resistance, we obtained its genomic sequences from two susceptible mutant lines, 1338-8-S1 and 1338-8-S4, by PCR followed by Sanger sequencing. Line 1338-8-S1 contained a 1-bp deletion in the CC domain of *Pm12-can* that led to a frameshift and the formation of a truncated protein. Line 1338-8-S4 contained a missense mutation in the Kinase-2 motif of the NBS domain of *Pm12-can*. We also carried out mutation analysis of 15 independent susceptible mutant lines (1338-8-S5 to 1338-8-S19) identified from 1206 EMS-induced M$_2$ families (Figure 2A). Each mutant contained a single base change in the coding region of *Pm12-can*. Two mutations caused premature stop codons, and the other 13 mutations led to amino acid changes in the CC domain (1), the linker between the CC and NBS domains (1), the Kinase-3a (RNBS-B) motif (1), the RNBS-C motif (2), the region close to the GLPL motif (1) of the NBS
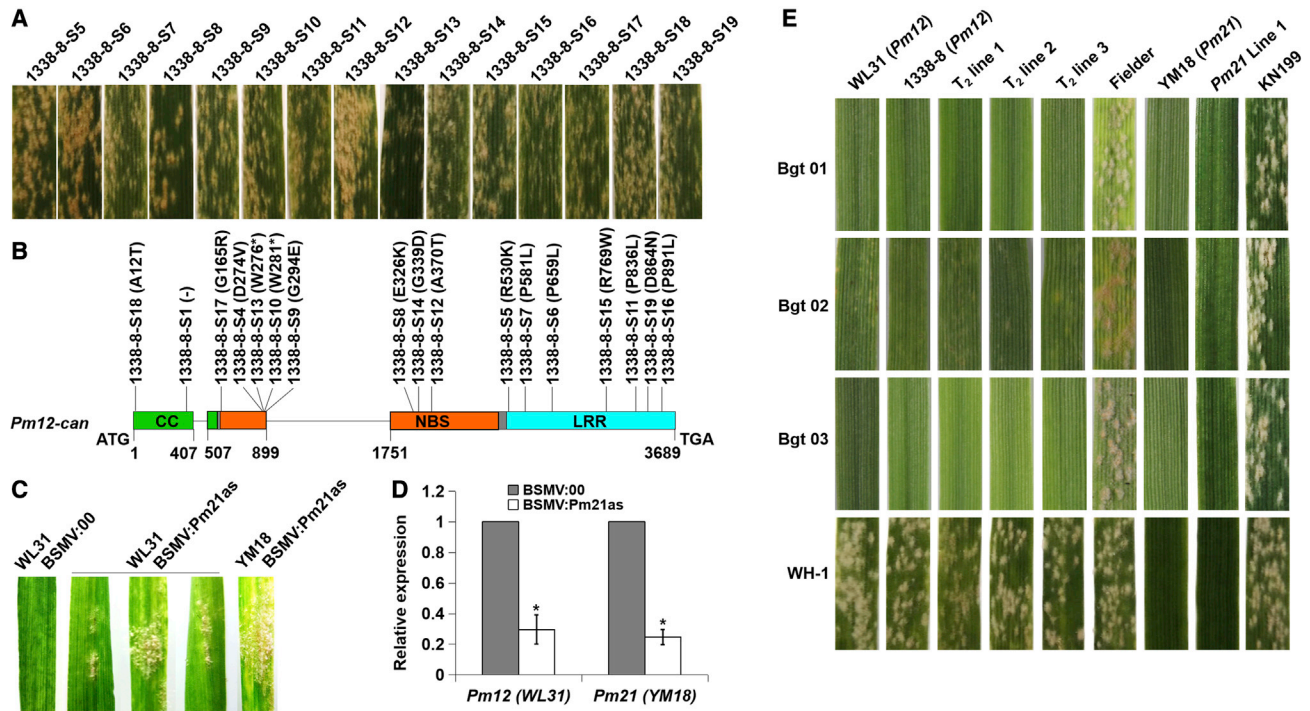
Figure 2. Functional validation of *Pm12*.

(A) Responses of EMS-induced mutants to Bgt01 at the seedling stage, using 1338-8 and YM9 as the resistant and susceptible controls, respectively, whose images can be found in Figure 1A.

(B) Gene structure showing mutation sites identified in susceptible mutants. The green, brown, and blue boxes are the CC, NBS, and LRR domains, respectively.

(C) Macroscopic phenotypes of the resistant wheat WL31 (carrying *Pm12*) after treatment with BSMV:Pm21as. BSMV:Pm21as-infected YM18 (carrying *Pm21*) and BSMV:00 (with empty vector)-infected WL31 were used as the positive and negative controls, respectively.

(D) Silencing efficiencies of *Pm12* in WL31 leaves and *Pm21* in YM18 leaves measured by qPCR. Error bars represent the standard error of the mean of three independent experiments. Statistical significance of differences was assessed using Student's *t*-test. *$P < 0.001$.

(E) Responses of T_2 transgenic lines expressing *Pm12* to four *Bgt* isolates at the one-leaf stage, using *Pm12* donors WL31 and 1338-8 as the resistant controls and the recipient Fielder as the susceptible control. The responses of *Pm12* plants were also compared with those of YM18, the transgenic wheat line (*Pm21* Line 1) carrying *Pm21*, and KN199 without any powdery mildew resistance gene.

domain, and the LRR domain (7) (Figure 2B). We also amplified and sequenced the *DvRGA1-like* gene, *AesRGA1*, in each mutant line and found no mutations. The fact that mutations were found only in *Pm12-can* strongly supports the notion that *Pm12-can* is actually the gene that controls *Pm12*-mediated resistance.

The VIGS approach was also used to test whether *Pm12-can* was required for *Pm12* resistance. In our previous work, the recombinant virus BSMV:Pm21as carrying a 362-bp LRR-encoding sequence that shares 94.2% nucleotide identity with that of *Pm12-can* effectively blocked *Pm21* resistance (He et al., 2018). Here, we found that infection of the resistant line WL31 with the BSMV:Pm21as construct compromised its *Pm12* resistance and allowed the development of *Bgt* colonies with disease symptoms and fungal sporulation on the leaves (Figure 2C and 2D). Taken together, these data indicate that the candidate gene *Pm12-can* is required for *Pm12*-mediated resistance to wheat powdery mildew.

Pm12-can confers highly effective resistance to powdery mildew in transgenic wheat lines

To validate the resistance function of *Pm12-can*, a construct harboring *Pm12-can* cDNA driven by the maize *ubi* promoter

was transformed into the susceptible wheat cv. Fielder using *Agrobacterium*-mediated transformation. Three of the four regenerated T_0 plants were confirmed to carry *Pm12-can* (Supplemental Figure 4). The T_2 plants derived from these three lines showed strong resistance to 122 *Bgt* isolates with infection type (IT) 0 or 1, with the exception of isolate WH-1. The responses of the transgenic plants from each line to the same isolate were consistent with those of the donors WL31 and 1338-8 (Figure 2E, Supplemental Table 3). Therefore, we concluded that *Pm12-can* is indeed *Pm12*. As a comparison, we also determined the disease responses of YM18 carrying *Pm21* and *Pm21* T_5 Line 1 (transgenic wheat line expressing *Pm21*) to the same set of *Bgt* isolates. The results showed that *Pm21* conferred immunity to all 123 isolates tested. This finding suggested that there is a difference in race specificity between *Pm12* and *Pm21*, which might be associated with the sequence variations in their LRR domains.

PM12 and PM21 differ in cell death-inducing activity caused by their different intramolecular structures

Cell death in *Nicotiana benthamiana* induced by overexpression of NLR proteins, such as MLA10, SR33, SR35, Rp1-D21, RGA4, and PM60, has been widely reported (Bai et al., 2012; Cesari et al.,
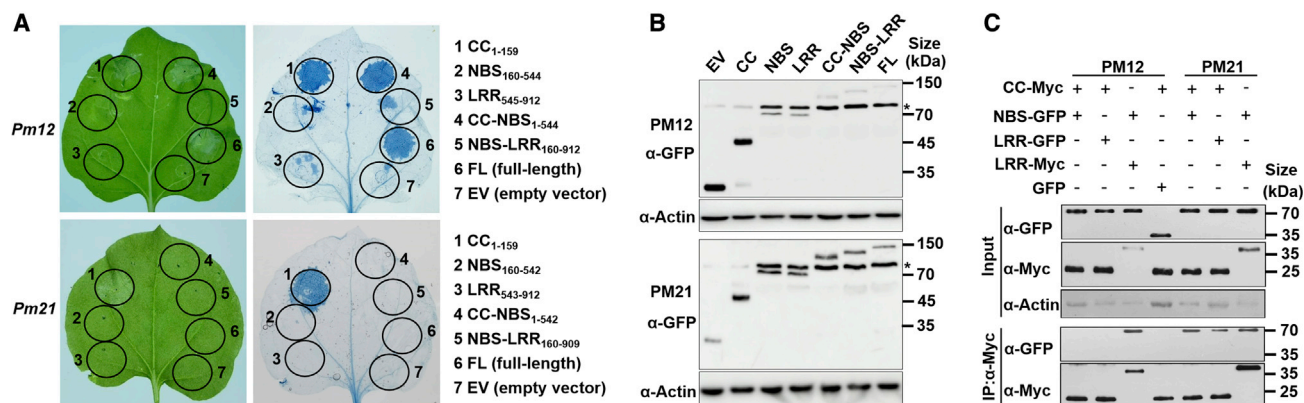
Figure 3. Cell death assay and Co-IP analysis in *N. benthamiana* leaves.
(A) Comparative analyses of cell death-inducing activities of the single or combined domain(s) encoded by *Pm12* and *Pm21*. *N. benthamiana* leaves were infiltrated with agrobacteria carrying different constructs. Cell death was observed by trypan blue staining at 48 h post infiltration.
(B) Western blotting detection of different domains or proteins expressed in *N. benthamiana* leaves. EV: empty vector. FL: full-length proteins. Tagged proteins were detected by western blotting with anti-GFP antibodies (α-GFP).
(C) Comparative analyses of interactions of different domains encoded by *Pm12* and *Pm21*. Different domains fused to GFP or Myc tags were transiently co-expressed in *N. benthamiana* leaves in the indicated combinations (+, agro-infiltrated construct; −, non-infiltrated construct), and total proteins were extracted at 20 h post infiltration. Tagged proteins were detected by western blotting in the input and after immunoprecipitation with anti-Myc antibodies (α-Myc). Actin was used as the protein loading control. Asterisk indicates non-specific signals.

2014, 2016; Wang et al., 2015; Zou et al., 2018). However, several studies have shown that different NLR-type powdery mildew resistance proteins identified from wheat crops may have different cell death-inducing activities (Bourras et al., 2015; Hewitt et al., 2021; Müller et al., 2022; Praz et al., 2016; Zou et al., 2018). To assess the cell death-inducing activities of PM12 and PM21, we infiltrated *Pm12* and *Pm21* into *N. benthamiana* leaves; overexpression of PM12 resulted in strong cell death, but overexpression of PM21 did not. We then detected the cell death-inducing activities of their CC, NBS, and LRR domains as well as the fragments CC-NBS and NBS-LRR. The PM12 and PM21 CC domains were able to induce cell death, whereas the other single domains were not (Figure 3A and 3B), indicating that the CC domains of both PM12 and PM21 are sufficient to trigger cell death. Interestingly, the PM12 CC-NBS fragment elicited a strong cell death response, whereas the PM21 CC-NBS fragment did not induce cell death. These findings suggest that the activities of the CC domains of PM12 and PM21 are intramolecularly regulated in different ways. Different domains of an NLR protein usually interact with each other, and cell death activity may be regulated by other domains in the same protein (Moffett et al., 2002; Rairdan et al., 2008; Wang et al., 2015, 2019a, 2019b; Bernoux et al., 2016; El Kasmi et al., 2017; Zhao et al., 2022). The above results prompted us to speculate that differences in cell death caused by full-length PM12 and PM21 might be caused by differences in regulation and interactions of the domains in the two proteins.

To test this hypothesis, co-immunoprecipitation (Co-IP) assays were performed on *N. benthamiana* leaves by co-expressing either NBS-GFP or LRR-GFP with CC-Myc of PM12 or PM21, followed by pull-down experiments with anti-GFP antibody (αGFP). The results showed that PM21 CC-Myc co-immunoprecipitated with both PM21 NBS-GFP and PM21 LRR-GFP, whereas PM12 CC-Myc did not co-immunoprecipitate with either PM12 NBS-GFP or PM12 LRR-GFP. Co-IP assays also revealed that both

PM12 and PM21 NBS domains interacted with their LRR domains (Figure 3C). Combining the cell death assays and Co-IP data, we suggest that differences in cell death-inducing activities of PM12 and PM21 likely resulted from differences in their intramolecular domain interactions.

Genomic data reveal the origin and evolutionary dynamics of the *Pm12/Pm21* loci in Triticeae species

In *D. villosum*, both *Pm21* (*DvRGA2*) and the immediately adjacent gene, *DvRGA1*, encode NLR proteins. Similarly, *Pm12* is also linked to the *DvRGA1-like* gene *AesRGA1* in *Ae. speltoides*. Using BLAST searches, we found frequent occurrences of this NLR gene pair in the genomes of Triticeae species, including common wheat, durum wheat, wild emmer, *T. urartu*, *Ae. tauschii*, and *Ae. speltoides* (Figure 4). Based on their location proximity and their high sequence similarity, the two genes in the pair are likely to be paralogs derived from a tandem duplication event in the Triticeae genomes. In the syntenic region of the *Brachypodium distachyon* genome, there are three tandemly duplicated copies of *DvRGA1-like* genes (*Bradi3g03874*, *Bradi3g03878*, and *Bradi3g03882*) that share 71.4%–72.9% identity and the same exon–intron organization as *DvRGA1*. However, no *DvRGA1-like* gene appears in rice (*Oryza sativa*), maize (*Zea mays*), and sorghum (*Sorghum bicolor*). This suggests that *DvRGA1-like* genes existed before the separation of *Brachypodium* and the Triticeae lineage. Furthermore, there is no *DvRGA2-like* gene near the *DvRGA1-like* gene or elsewhere in the *Brachypodium* genome, indicating that the *Pm21/Pm12* orthologs originated after the divergence of wheat species and *Brachypodium* but before the divergence of *D. villosum* and the common ancestor of the three wheat donor species *T. urartu* (A subgenome), *Ae. speltoides* (B subgenome), and *Ae. tauschii* (D subgenome).

Sequence analysis showed that the *DvRGA1* orthologs shared 96.4%–100% identity with each other; however, the
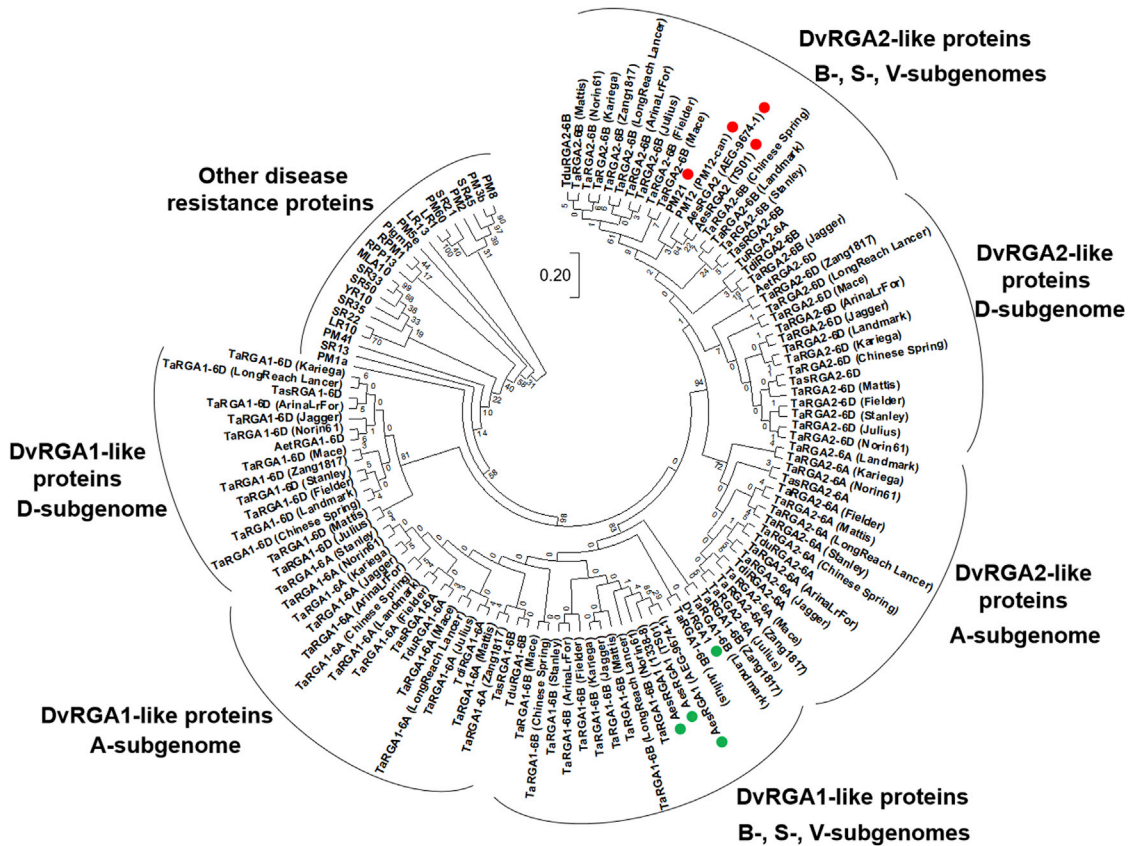
Figure 4. Phylogenetic tree of PM12 (PM12-can) and relevant NLR proteins from wheat species, rice, and *Arabidopsis*.
The phylogenetic tree was constructed based on full-length NLR proteins by the neighbor-joining method with the Poisson model in MEGA7 software.
Arabidopsis RPP13 was used to root the tree. The scale bar indicates an evolutionary distance of 0.20 amino acid substitutions per site. Red and green
dots indicate DvRGA2-like (including PM21 and PM12) and DvRGA1-like NLR proteins, respectively, from *D. villosum* and *Ae. speltoides*. Aet: *Ae.
tauschii*. Aes: *Ae. speltoides*. Dv: *D. villosum*. Ta: *Triticum aestivum* (common wheat). Tas: *T. aestivum* ssp. *spelta* (spelta wheat). Tdi: *T. dicoccoides* (wild
emmer). Tdu: *T. durum* (durum wheat). Tu: *T. urartu*. Wheat cultivars or related accessions are shown in brackets.

transcribed or predicted coding sequences of *Pm12/Pm21*
(*DvRGA2-like*) orthologs had only 72.0%–100% identity. This
indicates that *DvRGA1-like* genes are relatively conserved in
wheat and its related species, whereas *Pm12/Pm21* orthologs
are more evolutionarily dynamic. The *DvRGA1-like* gene has a
single intron (250–355 bp) that lies at the immediate N terminus
of the sequence encoding the Kinase-2 motif in the NBS
domain. *Pm12/Pm21* orthologs have three exons and two
introns. The first intron is very short (only 96–101 bp) and
lies upstream of the sequence encoding the NBS domain.
The second intron lies in the same location as that of the
DvRGA1-like genes. Compared with *Pm21* and *Pm12*, the
second introns of the orthologs *TaRGA2-6A*, *TaRGA2-6B*,
and *TaRGA2-6D*, derived from the wheat A, B, and D subge-
nomes, respectively, have clearly expanded, probably through
independent insertion events of different transposable ele-
ments (TEs) and/or other unknown repetitive elements (REs).
Further analysis at the subgenome level showed that most of
the intron expansion events in the *Pm12/Pm21* orthologs of
common wheat cv. Chinese Spring could be clearly traced
back to its tetraploid and diploid ancestral species, including
durum wheat, wild emmer, *T. urartu*, and *Ae. tauschii*
(Figure 5A).

The expressed *Pm12/Pm21* orthologs in Chinese Spring do not confer resistance to *Bgt*

The insertion of multiple TEs in the second intron was originally
thought to disrupt the expression of *Pm12/Pm21* genes in Chi-
nese Spring wheat. However, a search of the wheat expression
database (http://www.wheat-expression.com) revealed that
TaRGA2-6A, *TaRGA2-6B*, and *TaRGA2-6D* are all transcribed,
and their full-length open reading frame (ORF) sequences were
identified as *TraesCS6A02G120000.1*, *TraesCS6B02G148400.1*,
and *TraesCS6D02G110000.1*, respectively. qPCR analysis
confirmed that, despite the large expansion of the second intron,
the three orthologs could still be transcribed in Chinese Spring.
However, their transcript levels were significantly lower than
those of *Pm12* and *Pm21* during invasion by the *Bgt* isolate
Bgt01 (YZ01) (Figure 5B). Transcriptional analysis also indicated
that *TaRGA2-6A* and *TaRGA2-6B* were spliced in a similar
manner to *Pm12* and *Pm21*. We also performed single-cell tran-
sient assays to test whether overexpression of *Pm12/Pm21* or-
thologs provides resistance functions. The haustorium indexes
of *TaRGA2-6A*, *TaRGA2-6B*, and *TaRGA2-6D* were 81.8%,
75.4%, and 78.2%, respectively, significantly greater than
that of *Pm12* (42.3%) and similar to that of the negative
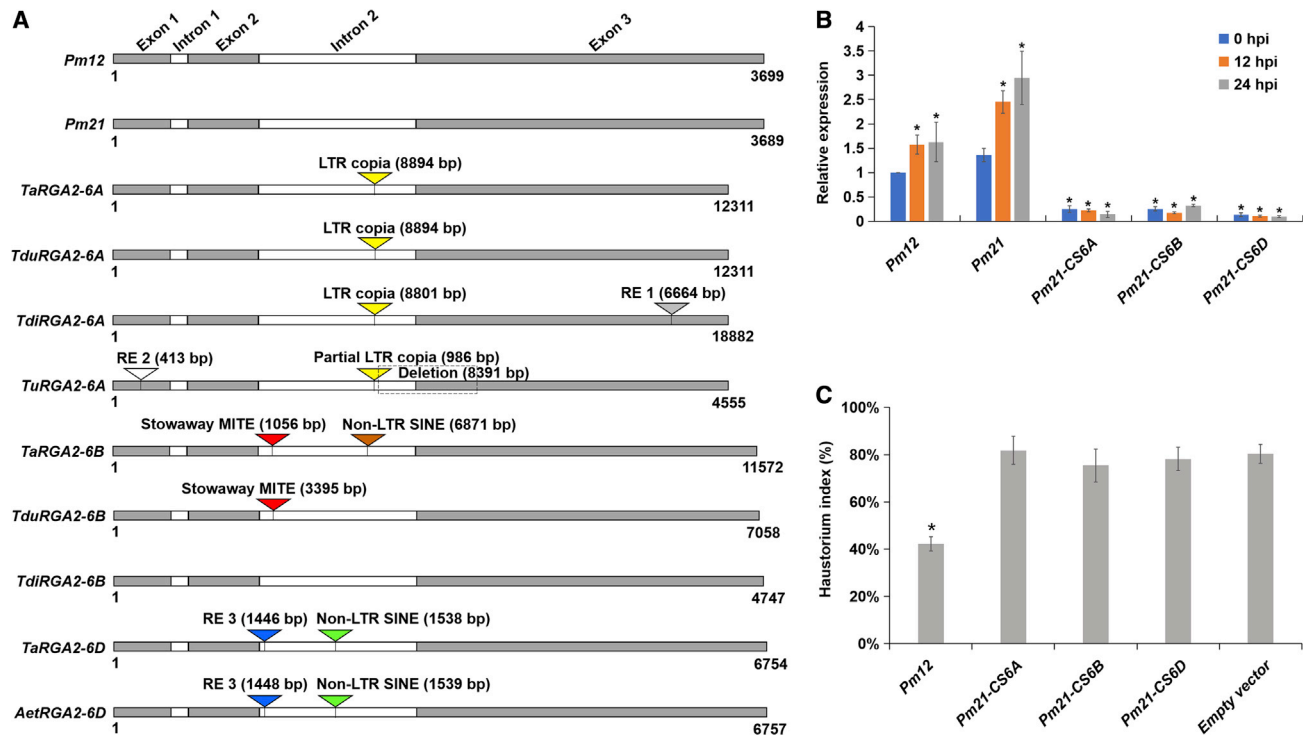control (80.3%) (Figure 5C). These results indicated that

Figure 5. Evolutionary, transcriptional, and transient expression analyses of *Pm12/Pm21* orthologs from wheat species.
(A) Gene structures of *Pm12/Pm21* orthologs in common wheat and its diploid and tetraploid ancestral species. Triangles with different colors represent different transposable elements (TEs) and repetitive elements (REs). The *Pm12/Pm21* orthologs *TaRGA2-6A*, *TaRGA2-6B*, and *TaRGA2-6D* were identified from wheat cv. Chinese Spring, *TduRGA2-6A* and *TduRGA2-6B* from *T. durum* (durum wheat), *TdiRGA2-6A* and *TdiRGA2-6B* from *T. dicoccoides* (wild emmer), *TuRGA2-6A* from *T. urartu*, and *TduRGA2-6D* from *Ae. tauschii*.
(B) qPCR analysis of *Pm12/Pm21* orthologs *TaRGA2-6A*, *TaRGA2-6B*, and *TaRGA2-6D* in Chinese Spring leaves. The leaves were inoculated with Bgt01 and sampled at 0, 12, and 24 h post inoculation (hpi). The relative expression levels of *TaRGA2-6A*, *TaRGA2-6B*, and *TaRGA2-6D* were compared with those of *Pm12* and *Pm21*.
(C) Single-cell transient expression assay of *TaRGA2-6A*, *TaRGA2-6B*, and *TaRGA2-6D* in wheat leaves. The vector expressing *Pm12* and the corresponding empty vector pUBI were used as the positive and negative controls. Statistical significance of differences was assessed using Student's *t*-test. *$P < 0.01$.

overexpression of the three Chinese Spring orthologs could not confer *Bgt* resistance, suggesting that accumulated variations in the coding regions likely led to loss of function.

DISCUSSION

Alien disease resistance genes from wild relatives usually confer high resistance to wheat diseases. However, after transfer into cultivated wheat, most of them have not been well utilized in breeding programs because of linkage drag that is difficult to overcome. The best way to use such genes is to clone them and transfer them directly into elite wheat lines using transgenic technology (Wulff and Moscou, 2014; Sánchez-Martín and Keller, 2019). However, owing to suppressed recombination between wheat and alien chromatins, it is difficult to isolate the alien genes in a wheat background using a positional cloning strategy based on genetic mapping. Here, we demonstrate an efficient strategy for physical mapping and identification of the alien powdery mildew resistance gene *Pm12* using mutants obtained by irradiation. EMS treatment is useful for creating mutations, but most mutations involve single-base variations rather than deletions within chromosomes (He et al., 2018). By contrast, we found that irradiation is a powerful tool for the

development of new genetic stocks with significant chromosomal aberrations (Zhang et al., 2015). Consequently, we proposed that irradiation would create more deletion mutations at the chromosome level. Such chromosomal deletions could easily be detected using traditional marker analysis and used for physical mapping of genes of interest. In the present study, two of four susceptible mutants of *Pm12* derived from the irradiated population were shown to have lost large chromosomal fragments, which enabled precise mapping of *Pm12*. Subsequently, another two irradiated susceptible mutants without chromosomal deletion in the target region were used to identify the candidate gene for *Pm12*. Thus, we successfully isolated the alien gene *Pm12*. The above strategy, based on irradiation-induced mutants, is fast and efficient for mapping and cloning of alien genes in a wheat background. The efficient cloning of effective alien genes can not only accelerate their application in breeding but also enable understanding of their functions and mechanisms.

In the *Pm21* locus of *D. villosum*, only one of the two paralogous NLR genes *DvRGA2 (Pm21)* and *DvRGA1* participates in powdery mildew resistance (He et al., 2018). Here, we showed that *Pm12*, the orthologous gene of *Pm21* in *Ae. speltoides*, is also

sufficient for resistance, independent of the adjacent gene *AesRGA1*. Interestingly, this NLR pair exists not only in *D. villosum* and *Ae. speltoides* but also in other published Triticeae genomes, including those of common wheat, wild emmer (*T. dicoccoides*), durum wheat (*T. durum*), *T. urartu*, and *Ae. tauschii*. The NLR pair does not appear in *Brachypodium*, rice, maize, and sorghum; however, *DvRGA1-like* genes can be found within a cluster in the orthologous region of *Brachypodium*. We suggest that *DvRGA1-like* NLRs appeared in the common ancestor of wheat and *Brachypodium*, whereas *DvRGA2-like* (*Pm12/Pm21-like*) NLRs might be duplicated from non-functional *DvRGA1-like* NLRs after the divergence of wheat and *Brachypodium*. Subsequently, the duplicated copies might have experienced more rapid evolution and gained resistance against powdery mildew diseases.

In the three *Pm12/Pm21* orthologs of the Chinese Spring genome, independent insertions of TEs and other REs occurred in the second intron. The insertions in the A and D subgenomes of wheat can be traced back directly to their diploid progenitors, *T. urartu* and *Ae. tauschii*, respectively, indicating that these insertion events occurred after the divergence of the two diploid progenitors. In the B subgenome of Chinese Spring, there are two insertions in the *Pm12/Pm21* ortholog. The first insertion (Stow-away MITE) is also found in durum wheat but not in wild emmer, whereas the other (RE 1) is not found in either durum wheat or wild emmer. *Ae. speltoides* is considered to be the donor of the wheat B subgenome, and *Pm12*, which originated from *Ae. speltoides*, does not have a large insertion in its second intron. A number of TE insertion events that appeared to decrease the transcript levels of the corresponding genes were reported in intronic regions of the *Ae. tauschii* genome (Zhao et al. 2017). Here, we also showed that insertions of large fragments significantly decreased the transcript levels of the three *Pm12/Pm21* orthologs in Chinese Spring, which were only 13.4%–25.6% of those of *Pm12* and *Pm21*. In the VIGS experiment, transcript levels of *Pm12* and *Pm21* were reduced to 29.6% and 24.7%, respectively, making resistant plants susceptible to powdery mildew. Therefore, the reduced transcript levels of the orthologs caused by insertion events may have undermined resistance. Furthermore, transient overexpression revealed that the three orthologs from susceptible wheat cv. Chinese Spring did not provide resistance to powdery mildew. Hence, we conclude that the loss of function of the three Chinese Spring orthologs is most likely caused by both insertion events and sequence variations accumulated in their coding regions.

The functional *Pm12* and *Pm21* resistance genes identified in the two diploid wild species, *Ae. speltoides* and *D. villosum*, respectively, have undoubtedly undergone independent evolution in different environments since divergence from their common ancestral gene. The two orthologous resistance genes now share 89.9% nucleotide sequence identity and 84.9% amino acid sequence identity. A total of 135 amino acid variations were found in different domains of the two proteins, 16 of which involve the solvent-exposed residues of the LRR motifs. We observed that *Pm12* and *Pm21* showed different responses to isolate WH-1, suggesting that there are differences in race specificity between the two orthologous genes. We propose that this difference may result from the variations in the solvent-exposed residues of the LRR motifs, as they are considered to be responsible for percep-

tion of the pathogen effector (Wulff et al., 2009; He et al., 2020). From another point of view, a key effector in WH-1 might have obtained new variation(s), leading it to escape recognition by PM12 but still be perceived by PM21. It would be interesting to investigate whether the two orthologous NLR proteins perceive the same effector and how the isolate WH-1 escapes from PM12 but not from PM21.

In general, NLRs must be strictly regulated in the absence of their cognate pathogen effectors to avoid autoimmunity that would be damaging to the host. Previous studies have shown that some NLRs, including SR33, SR50, Rp1-D21, and RGA4, can induce pathogen effector-independent cell death when transiently over-expressed in *N. benthamiana* (Cesari et al., 2014, 2016; Wang et al., 2015), suggesting that these NLRs are in an autoactive state. However, other NLRs, such as Rx, RPM1, and ZAR1 (Bendahmane et al., 2002; Baudin et al., 2017; El Kasmi et al., 2017), do not lead to cell death, indicating that they are in an autoinhibited state. In the present study, the full-length forms of PM12 and PM21 showed obvious differences in cell death activity. This result suggests that in the absence of a pathogen effector, PM21 is present in an autoinhibited state, whereas PM12 is autoactive.

Previous transient overexpression assays have demonstrated the complexity of the autoinhibited/autoactive states of NLR-type powdery mildew resistance proteins of wheat crops. For instance, *T. urartu* PM60 can induce cell death (Zou et al., 2018), whereas wheat PM1, PM2, PM3, and PM17 cannot (Bourras et al., 2015; Praz et al., 2016; Hewitt et al., 2021; Müller et al., 2022). Furthermore, some NLRs encoded by alleles with high sequence identity also have different cell death-inducing activity. For instance, overexpression of MLA10 from barley (*Hordeum vulgare*) can lead to cell death, whereas overexpression of MLA1 and MLA6 does not (Bai et al., 2012; Bauer et al., 2021). Confusingly, MLA10 showed no cell death activity in the report of Bauer et al. (2021). Intramolecular interactions in NLRs commonly play crucial roles in stabilizing active or autoinhibited protein conformations (Rairdan et al., 2008; Wang et al., 2015, 2019a; El Kasmi et al., 2017; Zhao et al., 2022). Co-IP assays revealed that interaction occurs between the PM21 CC domain and its NBS and LRR domains but not between the PM12 CC domain and its NBS or LRR domains.

Because PM12 and PM21 show a relatively high number of amino acid differences, we believe that differences in their intramolecular interactions must be generated by their sequence variations. These sequence variations may also alter their effector recognition. It will be very interesting to determine which of the amino acid differences influence recognition and which influence activity leading to altered cell death signaling. Future work involving structural characterization and functional experiments in wheat protoplasts will further our understanding of these molecular mechanisms.

METHODS

Plant materials and growth conditions

The common wheat–*Ae. speltoides* translocation Wembley Line #31 (WL31, 6BS-6SS.6SL), originally generated at the John Innes Centre, Nor-wich, UK, is the donor of *Pm12* (Miller et al., 1988; Jia et al., 1996). The

resistant introgression line 1338-8 was derived from WL31 (Song et al., 2007). Wheat cv. Chinese Spring was provided by the Germplasm Resources Information Network (GRIN). The resistant wheat cv. Yangmai 18 (YM18) carrying *Pm21* on the translocated chromosome T6AL.6VS and the susceptible cv. Yangmai 9 (YM9) were both developed at Yangzhou Academy of Agricultural Sciences, Yangzhou, China. The susceptible cv. Fielder was used as the recipient for genetic transformation. *Pm21* T$_5$ Line 1, a transgenic wheat line expressing *Pm21*, was originally developed in our previous work (He et al., 2018). Kenong 199 (KN199), the recipient for *Pm21* transformation, is a highly susceptible wheat variety without any *Pm* genes. *Nicotiana benthamiana* was used for transient expression assays. Plants were grown in a greenhouse with LED lighting under long-day conditions (16 h light/8 h dark) at 24°C.

Evaluation of powdery mildew resistance

Three seedlings of each line at the one-leaf stage were inoculated with *Bgt* isolates by dusting fungal conidiospores onto leaves. The inoculated plants were grown under a daily cycle of 16 h light/8 h dark at 24°C in a greenhouse. Responses to powdery mildew were evaluated at 7–10 days after inoculation. The responses of transgenic wheat to *Bgt* pathogens were assessed using two sets of *Bgt* isolates collected from different regions of China. The first set contained 22 isolates maintained by Dr. Pengtao Ma at Yantai University (He et al., 2021b), and the second set included 100 isolates held by the Institute of Plant Protection and Soil Science, Hubei Academy of Agricultural Sciences (Bourras et al., 2019). Isolate WH-1 was newly collected from Wuhan, China. Infection types were scored on a 0 to 4 scale as described by An et al. (2013), where ITs 0, 1, and 2 were regarded as resistant and ITs 3 and 4 as susceptible.

Genomic DNA isolation and molecular marker analysis

Genomic DNA was isolated from the leaves of seedlings using the TE-boiling method (He et al., 2017). A total of 50 markers, including 46 *D. villosum* 6VS-specific markers reported previously (Song et al., 2009; Qi et al., 2010; Bie et al., 2015a, 2015b; He et al., 2016, 2017; Zhu et al., 2018) and four new markers developed in this study using the CISP (conserved-intron scanning primers) strategy (He et al., 2013) based on the potential collinearity relationship between *Ae. speltoides* 6SS and *D. villosum* 6VS, were used to screen for polymorphisms among YM9, WL31, and 1338-8. The diagnostic molecular marker *6SS-04* was designed based on the promoter sequences of *Pm12* and *Pm21*. PCR products were separated on an 8% non-denaturing polyacrylamide gel, followed by silver staining. All polymorphic DNA markers for 6SS are listed in Supplemental Table 1. In the physical map, the order of molecular markers was adopted from the reference genome of *Ae. speltoides* accession AEG-9674-1 (Avni et al., 2022).

Isolation of the candidate gene for *Pm12* (*Pm12-can*)

Three primer pairs were used to isolate the genes or fragments at the *Pm12* locus. The first pair, *Pm12*-I-1, was designed according to *D. villosum DvRGA1* and used to isolate a *DvRGA1-like* gene from genomic DNA of the line WL31. The second pair, *Pm12*-I-2, was designed based on the conserved sequences of *Pm21* alleles reported previously (He et al., 2020) and used to amplify the DNA fragment that covered most of the coding sequence of *Pm12-can*, the candidate for *Pm12*. The third primer pair, *Pm12*-I-3, was designed based on the terminus of *DvRGA1* and the head of *Pm21* and was used for isolating the intergenic region between the two genes. Subsequently, the downstream sequence of *Pm12-can* was obtained by thermal-asymmetric-interlaced (TAIL) PCR (Liu and Huang, 1998). The genomic sequence of the *Pm12* locus was then assembled, and the corresponding cDNA sequences of the two genes were confirmed by reverse transcriptase (RT)–PCR. The high fidelity PrimeSTAR Max Premix (TaKaRa, Japan) was used for all PCR amplification. All primers used in this study are listed in Supplemental Table 4.

RT–PCR and quantitative RT–PCR analyses

Total RNA was extracted from the first fully expanded leaves of seedlings from lines WL31, 1338-8, Yangmai 18, and Chinese Spring, with or without Bgt01 inoculation, using the TRIzol reagent (Life Technologies, Carlsbad, CA, USA). Two micrograms of total RNA were used for synthesis of first-strand cDNA using the PrimeScript II 1st Strand cDNA Synthesis Kit (TaKaRa, Shiga, Japan). qPCR was performed on an ABI 7300 Real Time PCR System (Life Technologies, Carlsbad, CA, USA) as previously described (He et al., 2016). The wheat actin gene was used as the reference gene (Bahrini et al., 2011). When performing qPCR analysis, three independent biological replicates of each line were used. Statistical significance of differences was assessed using Student's *t*-test.

Sequence analysis

Pm12 was used to perform BLAST searches against the genomes of durum wheat cv. Svevo (Maccaferri et al., 2019), wild emmer accession Zavitan (Avni et al., 2017), *T. urartu* accession G1812 (Ling et al., 2018), *Ae. tauschii* accession AL8/78 (Luo et al., 2017), *Ae. speltoides* accessions AEG-9674-1 and TS01 (Avni et al., 2022; Li et al., 2022), and multiple wheat cultivars (International Wheat Genome Sequencing Consortium et al., 2018; Guo et al., 2020; Walkowiak et al., 2020; Sato et al., 2021). The matched sequences with the highest identities from homeologous group 6 of wheat species were considered to be *Pm12/Pm21* orthologs whose exon–intron structures were predicted according to those of *Pm12* and *Pm21*. The *DvRGA1*-like and *DvRGA2*-like sequences were also obtained from the above genomes after BLAST analysis and annotated based on the expression data of *DvRGA1* and *DvRGA2* from *D. villosum* (He et al., 2018). TEs were predicted by comparison with the TREP database (https://trep-db.uzh.ch). Other DNA REs were found by BLAST searches against the reference genome of wheat cv. Chinese Spring (RefSeq v1.1). Nucleotide and amino acid sequence identities were calculated with DNASTAR software (Burland 2000). Protein domain prediction and multiple sequence alignment were performed with SMART (Letunic et al., 2015) and CLUSTAL W (Thompson et al., 1994), respectively. Annotation of LRR motifs was performed as described in our previous work (He et al., 2020). The phylogenetic tree was constructed based on the (putative) full-length proteins by the neighbor-joining method with the Poisson model in MEGA7 software (Kumar et al., 2016).

Barley stripe mosaic virus-induced gene silencing (BSMV-VIGS) analysis

BSMV-VIGS was used to perform a transient assay to investigate the potential functional relationship between *Pm12* and *Pm21*. The recombinant virus BSMV:Pm21as (syn. BSMV:DvRGA2as) harboring the DNA fragment of the *Pm21* gene was used to infect the leaves of WL31 carrying *Pm12*. BSMV:Pm21as-infected YM18 (harboring *Pm21*) and BSMV:00 (harboring empty vector)-infected WL31 were used as positive and negative controls, respectively. At 6 days, the virus-infected leaves were challenged with the avirulent isolate Bgt01. At 5 days after *Bgt* inoculation, the powdery mildew reactions were observed. Details of the silencing test are described in our previous work (He et al., 2016, 2018).

Mutation analysis

About 500 dry seeds of the powdery mildew-resistant line 1338-8 that were harvested in the most recent season and had a high germination rate were exposed to ^{60}Co-γ-ray irradiation with 200 Gy at a dosage rate of 1.0 Gy/min (Zhang et al., 2015). After irradiation, the seeds were sown immediately in the field, and 316 M$_2$ families were generated. Independently, ~2000 seeds of 1338-8 were treated with 0.6% EMS, resulting in 1206 M$_2$ families. About 100 individuals of each M$_2$ family were used to screen for susceptible mutants by inoculation with *Bgt* isolate Bgt01, which is avirulent to *Pm12*. The resistant line 1338-8 and the susceptible line YM9 were used as the controls. Susceptible mutants obtained by irradiation were then used for molecular marker analysis to test for potential chromosomal deletion. The candidate gene

Pm12-can in each mutant line was amplified from its genomic DNA using the primer pair Pm12-GT and subjected to Sanger sequencing. Each mutated *Pm12-can* gene was verified independently by sequencing the PCR product harboring the candidate mutation site. The *DvRGA1-like* gene in each mutant was also amplified by PCR and sequenced.

Plasmid construction

For wheat transformation, cDNA with the entire ORF of *Pm12-can* was cloned into the binary vector pLGY02 at the *Sma*I and *Spe*I sites. The resulting construct was designated pLGY02-*Pm12-can* and expressed the candidate gene under the control of a maize ubiquitin promoter. For single-cell transient assays in wheat, the *Pm12/Pm21* orthologs *Pm21-CS6A*, *Pm21-CS6B*, and *Pm21-CS6D* were amplified from wheat cv. Chinese Spring cDNA and individually cloned into the destination vector pUbi-GW using gene-specific primers with Gateway technology (Shen et al., 2007). As a positive control, *Pm12* was also inserted into the same vector. For transient assays in *N. benthamiana*, the coding sequences of *Pm12* and *Pm21* were amplified and inserted into the pS1300-GFP-Nos or pS1300-myc-Nos vector to create fusions with GFP or Myc tags at the C terminus. Genes on the constructs were driven by a constitutive promoter (Dong et al., 2018; Gao et al., 2020).

Wheat transformation

The construct pLGY02-*Pm12-can* was used to transform the susceptible wheat cv. Fielder by *Agrobacterium tumefaciens* (agrobacterium)-mediated transformation (Zhang et al., 2018). Both T_0 and T_1 plants were tested for the presence of the transgene by PCR amplification with primer pair Pm12-MA, and cv. Fielder was used as the negative control. Powdery mildew responses of three plants from each T_2 line were tested at the one-leaf stage after inoculation with different *Bgt* isolates.

Single-cell transient assay in wheat leaves

Single-cell transient expression assays were performed as described previously (Shen et al., 2007). In brief, a mixture of the construct expressing an individual *Pm12/Pm21* ortholog and the pUBI:GUS reporter construct was introduced into leaves of the susceptible wheat cv. KN199 by biolistic bombardment. After 4 h, the leaves were inoculated with *Bgt* isolate E18 (held by the lab of Dr. Qian-Hua Shen, Institute of Genetics and Developmental Biology, Chinese Academy of Sciences, China) for 48 h. Two days after inoculation, the leaves were GUS stained, and fungal structures were examined under a microscope. The haustorium index (i.e., the percentage of GUS-stained cells with haustoria among all GUS-stained cells invaded by *Bgt*) was used to assess whether the tested genes conferred resistance to powdery mildew. Constructs carrying *Pm12* or the empty vector were used as positive and negative controls, respectively.

Agroinfiltration of *N. benthamiana* leaves

Agrobacterium-mediated transient expression (agroinfiltration) was conducted as described in Liu et al. (2010) with minor modifications. In brief, the appropriate plasmid construct was transformed into *Agrobacterium* strain GV3101. The *Agrobacterium* strains were then grown to an optical OD_{600} of about 1.0. The cultures were harvested by centrifugation, resuspended in infiltration medium containing 2% sucrose, 0.5% MS, 10 mM MES (pH 5.6), and 200 μM acetosyringone, adjusted to an OD_{600} from 0.5 to 1, and incubated for 2–4 h at room temperature before infiltration. *N. benthamiana* leaves were used for infiltration. For co-expression of multiple proteins, agrobacteria carrying different constructs were mixed in a 1:1 ratio and used for infiltration. After infiltration, plants were maintained in growth chambers for subsequent assays.

Cell death assay on *N. benthamiana* leaves

The cell death assay was performed as described by Bai et al. (2012) and Gao et al. (2020). In brief, each *Agrobacterium* strain carrying a plasmid construct was infiltrated into a 1-cm circular region on five different leaves for three independent experiments. Leaves were photographed at 24–48 h after infiltration, soaked in trypan blue solution (10 ml lactic acid, 10 ml glycerol, 10 g phenol, 10 mg trypan blue, and 50 ml ethanol dissolved in 30 ml distilled water), and heated in a boiling water bath for 5 min. Leaves were then destained in 2.5 g ml^{-1} chloral hydrate solution until the background was clear.

Protein extraction, immunoblotting, and co-immunoprecipitation assay

Agrobacterium strain GV3101 carrying constructs expressing GFP- or Myc-fused proteins were mixed and infiltrated into *N. benthamiana* leaves as described above. Before cell death was visible (at about 20 h post infiltration), the total leaf proteins were extracted in 0.5 ml plant extraction buffer (CWBIO, Beijing, China), followed by centrifugation at 12 000 *g* for 20 min. Portions of the supernatants were saved as input samples for later SDS–PAGE and immunoblot analysis. For the Co-IP assay, the remaining supernatant was incubated with 4 μg of anti-Myc monoclonal antibody (Proteintech, Chicago, IL, USA) at 4°C for 2–4 h. The antibody–protein complexes were captured by incubation with 18 μl of agarose resin conjugated with protein A/G for 2–4 h at 4°C. After washing six times with IP buffer, the immunocomplexes were heated at 95°C for 5 min in 50 μl 1× SDS loading buffer. The supernatant after centrifugation was used for immunoblot analysis (Gao et al., 2020).

ACCESSION NUMBERS

The genomic sequence of *Pm12* has been deposited in GenBank under accession number MN334940.

SUPPLEMENTAL INFORMATION

Supplemental information can be found online at https://doi.org/10.1016/j.xplc.2022.100472.

AUTHOR CONTRIBUTIONS

H.H., A.G., and P.M. conceived and designed the research. S.Z., C.L., S.G., Z.C., R.C., T.L., R.L., H.D., R.G., G.L., M.L., R.F., and H.Z. performed experiments. S.Z., S.G., Z.L., Q.S., and H.H. analyzed the data. S.Z., C.L., S.G., A.G., P.M., and H.H. wrote the manuscript. All authors read and approved the final manuscript. S.Z., C.L., and S.G. contributed equally to this work.

REFERENCES

An, D., Ma, P., Zheng, Q., Fu, S., Li, L., Han, F., Han, G., Wang, J., Xu, Y., Jin, Y., et al. (2019). Development and molecular cytogenetic identification of a new wheat-rye 4R chromosome disomic addition line with resistances to powdery mildew, stripe rust and sharp eyespot. Theor. Appl. Genet. **132**:257–272.

An, D., Zheng, Q., Zhou, Y., Ma, P., Lv, Z., Li, L., Li, B., Luo, Q., Xu, H., and Xu, Y. (2013). Molecular cytogenetic characterization of a new wheat-rye 4R chromosome translocation line resistant to powdery mildew. Chromosome Res. **21**:419–432.

Avni, R., Lux, T., Minz-Dub, A., Millet, E., Sela, H., Distelfeld, A., Deek, J., Yu, G., Steuernagel, B., Pozniak, C., et al. (2022). Genome sequences of three *Aegilops* species of the section Sitopsis reveal phylogenetic relationships and provide resources for wheat improvement. Plant J. **110**:179–192.

Avni, R., Nave, M., Barad, O., Baruch, K., Twardziok, S.O., Gundlach, H., Hale, I., Mascher, M., Spannagl, M., Wiebe, K., et al. (2017). Wild emmer genome architecture and diversity elucidate wheat evolution and domestication. Science **357**:93–97.

Bahrini, I., Ogawa, T., Kobayashi, F., Kawahigashi, H., and Handa, H. (2011). Overexpression of the pathogen-inducible wheat *TaWRKY45* gene confers disease resistance to multiple fungi in transgenic wheat plants. Breed Sci. **61**:319–326.

Bai, S., Liu, J., Chang, C., Zhang, L., Maekawa, T., Wang, Q., Xiao, W., Liu, Y., Chai, J., Takken, F.L.W., et al. (2012). Structure-function analysis of barley NLR immune receptor MLA10 reveals its cell compartment specific activity in cell death and disease resistance. PLoS Pathog. **8**:e1002752.

Baudin, M., Hassan, J.A., Schreiber, K.J., and Lewis, J.D. (2017). Analysis of the ZAR1 immune complex reveals determinants for immunity and molecular interactions. Plant Physiol. **174**:2038–2053.

Bauer, S., Yu, D., Lawson, A.W., Saur, I.M.L., Frantzeskakis, L., Kracher, B., Logemann, E., Chai, J., Maekawa, T., and Schulze-Lefert, P. (2021). The leucine-rich repeats in allelic barley MLA immune receptors define specificity towards sequenceunrelated powdery mildew avirulence effectors with a predicted common RNase-like fold. PLoS Pathog. **17**:e1009223.

Bendahmane, A., Farnham, G., Moffett, P., and Baulcombe, D.C. (2002). Constitutive gain-of-function mutants in a nucleotide binding site-leucine rich repeat protein encoded at the *Rx* locus of potato. Plant J. **32**:195–204.

Bernoux, M., Burdett, H., Williams, S.J., Zhang, X., Chen, C., Newell, K., Lawrence, G.J., Kobe, B., Ellis, J.G., Anderson, P.A., and Dodds, P.N. (2016). Comparative analysis of the flax immune receptors L6 and L7 suggests an equilibrium-based switch activation model. Plant Cell **28**:146–159.

Bie, T., Zhao, R., Jiang, Z., Gao, D., Zhang, B., and He, H. (2015a). Efficient marker-assisted screening of structural changes involving *Haynaldia villosa* chromosome 6V using a double-distal-marker strategy. Mol. Breeding **35**:34.

Bie, T., Zhao, R., Zhu, S., Chen, S., Cen, B., Zhang, B., Gao, D., Jiang, Z., Chen, T., Wang, L., et al. (2015b). Development and characterization of marker *MBH1* simultaneously tagging genes *Pm21* and *PmV* conferring resistance to powdery mildew in wheat. Mol. Breeding **35**:189.

Bourras, S., Kunz, L., Xue, M., Praz, C.R., Müller, M.C., Kälin, C., Schläfli, M., Ackermann, P., Flückiger, S., Parlange, F., et al. (2019). The *AvrPm3-Pm3* effector-NLR interactions control both race-specific resistance and host-specificity of cereal mildews on wheat. Nat. Commun. **10**:2292.

Bourras, S., McNally, K.E., Ben-David, R., Parlange, F., Roffler, S., Praz, C.R., Oberhaensli, S., Menardo, F., Stirnweis, D., Frenkel, Z., et al. (2015). Multiple avirulence loci and allele-specific effector recognition control the *Pm3* race-specific resistance of wheat to powdery mildew. Plant Cell **27**:2991–3012.

Burland, T.G. (2000). DNASTAR's Lasergene sequence analysis software. Methods Mol. Biol. **132**:71–91.

Cao, A., Xing, L., Wang, X., et al. (2011). Serine/threonine kinase gene *Stpk-V*, a key member of powdery mildew resistance gene *Pm21*, confers powdery mildew resistance in wheat. Proc. Natl. Acad. Sci. USA **108**:7727–7732.

Césari, S., Kanzaki, H., Fujiwara, T., Bernoux, M., Chalvon, V., Kawano, Y., Shimamoto, K., Dodds, P., Terauchi, R., and Kroj, T. (2014). The NB-LRR proteins RGA4 and RGA5 interact functionally and physically to confer disease resistance. EMBO J. **33**:1941–1959.

Cesari, S., Moore, J., Chen, C., Webb, D., Periyannan, S., Mago, R., Bernoux, M., Lagudah, E.S., and Dodds, P.N. (2016). Cytosolic activation of cell death and stem rust resistance by cereal MLA-family CC-NLR proteins. Proc. Natl. Acad. Sci. USA **113**:10204–10209.

Chen, P., You, C., Hu, Y., Chen, S., Zhou, B., Cao, A., and Wang, X. (2013). Radiation-induced translocations with reduced *Haynaldia villosa* chromatin at the *Pm21* locus for powdery mildew resistance in wheat. Mol. Breeding **31**:477–484.

Dong, H., Bai, L., Zhang, Y., Zhang, G., Mao, Y., Min, L., Xiang, F., Qian, D., Zhu, X., and Song, C.P. (2018). Modulation of guard cell turgor and drought tolerance by a peroxisomal acetate-malate shunt. Mol. Plant **11**:1278–1291.

El Kasmi, F., Chung, E.H., Anderson, R.G., Li, J., Wan, L., Eitas, T.K., Gao, Z., and Dangl, J.L. (2017). Signaling from the plasma-membrane localized plant immune receptor RPM1 requires self-association of the full-length protein. Proc. Natl. Acad. Sci. USA **114**:E7385–E7394.

Gao, A., Hu, M., Gong, Y., Dong, R., Jiang, Y., Zhu, S., Ji, J., Zhang, D., Li, S., and He, H. (2020). Pm21 CC domain activity modulated by intramolecular interactions is implicated in cell death and disease resistance. Mol. Plant Pathol. **21**:975–984.

Gaurav, K., Arora, S., Silva, P., Sánchez-Martín, J., Horsnell, R., Gao, L., Brar, G.S., Widrig, V., John Raupp, W., Singh, N., et al. (2022). Population genomic analysis of *Aegilops tauschii* identifies targets for bread wheat improvement. Nat. Biotechnol. **40**:422–431.

Guo, W., Xin, M., Wang, Z., Yao, Y., Hu, Z., Song, W., Yu, K., Chen, Y., Wang, X., Guan, P., et al. (2020). Origin and adaptation to high altitude of Tibetan semi-wild wheat. Nat. Commun. **11**:5085.

He, H., Du, H., Liu, R., Liu, T., Yang, L., Gong, S., Tang, Z., Du, H., Liu, C., Han, R., et al. (2021a). Characterization of a new gene for resistance to wheat powdery mildew on chromosome 1RL of wild rye *Secale sylvestre*. Theor. Appl. Genet. **134**:887–896.

He, H., Ji, J., Li, H., Tong, J., Feng, Y., Wang, X., Han, R., Bie, T., Liu, C., and Zhu, S. (2020). Genetic diversity and evolutionary analyses reveal the powdery mildew resistance gene *Pm21* undergoing diversifying selection. Front. Genet. **11**:489.

He, H., Ji, Y., Zhu, S., Li, B., Zhao, R., Jiang, Z., and Bie, T. (2017). Genetic, physical and comparative mapping of the powdery mildew resistance gene *Pm21* originating from *Dasypyrum villosum*. Front. Plant Sci. **8**:1914.

He, H., Liu, R., Ma, P., Du, H., Zhang, H., Wu, Q., Yang, L., Gong, S., Liu, T., Huo, N., et al. (2021b). Characterization of *Pm68*, a new powdery mildew resistance gene on chromosome 2BS of Greek durum wheat TRI 1796. Theor. Appl. Genet. **134**:53–62.

He, H., Zhu, S., Jiang, Z., Ji, Y., Wang, F., Zhao, R., and Bie, T. (2016). Comparative mapping of powdery mildew resistance gene *Pm21* and functional characterization of resistance-related genes in wheat. Theor. Appl. Genet. **129**:819–829.

He, H., Zhu, S., Sun, W., Gao, D., and Bie, T. (2013). Efficient development of *Haynaldia villosa* chromosome 6VS-specific DNA markers using a CISP-IS strategy. Plant Breed. **132**:290–294.

He, H., Zhu, S., Zhao, R., Jiang, Z., Ji, Y., Ji, J., Qiu, D., Li, H., and Bie, T. (2018). *Pm21*, encoding a typical CC-NBS-LRR protein, confers broad-spectrum resistance to wheat powdery mildew disease. Mol. Plant **11**:879–882.

Hewitt, T., Müller, M.C., Molnár, I., Mascher, M., Holušová, K., Šimková, H., Kunz, L., Zhang, J., Li, J., Bhatt, D., et al. (2021). A highly differentiated region of wheat chromosome 7AL encodes a *Pm1a* immune receptor that recognises its corresponding *AvrPm1a* effector from *Blumeria graminis*. New Phytol. **229**:2812–2826.

Hurni, S., Brunner, S., Buchmann, G., Herren, G., Jordan, T., Krukowski, P., Wicker, T., Yahiaoui, N., Mago, R., and Keller, B. (2013). Rye *Pm8* and wheat *Pm3* are orthologous genes and show evolutionary conservation of resistance function against powdery mildew. Plant J. **76**:957–969.

International Wheat Genome Sequencing Consortium (IWGSC), IWGSC RefSeq Principal Investigators, Appels, R., Eversole, K., Feuillet, C., Keller, B., Rogers, J., Stein, N., IWGSC Whole-Genome Assembly Principal Investigators, Pozniak, C.J., et al. (2018). Shifting the limits in wheat research and breeding using a fully annotated reference genome. Science **361**:eaar7191.

Jia, J., Devos, K.M., Chao, S., Miller, T.E., Reader, S.M., and Gale, M.D. (1996). RFLP-based maps of the homoeologous group-6 chromosomes of wheat and their application in that tagging of *Pm12*, a powdery mildew resistance gene transferred from *Aegilops speltoides* to wheat. Theor. Appl. Genet. **92**:559–565.

Krattinger, S.G., Lagudah, E.S., Spielmeyer, W., Singh, R.P., Huerta-Espino, J., McFadden, H., Bossolini, E., Selter, L.L., and Keller, B. (2009). A putative ABC transporter confers durable resistance to multiple fungal pathogens in wheat. Science **323**:1360–1363.

Kumar, S., Stecher, G., and Tamura, K. (2016). MEGA7: molecular evolutionary genetics analysis version 7.0 for bigger datasets. Mol. Biol. Evol. **33**:1870–1874.

Letunic, I., Doerks, T., and Bork, P. (2015). SMART: recent updates, new developments and status in 2015. Nucleic Acids Res. **43**:D257–D260.

Li, L.F., Zhang, Z.B., Wang, Z.H., Li, N., Sha, Y., Wang, X.F., Ding, N., Li, Y., Zhao, J., Wu, Y., et al. (2022). Genome sequences of the five Sitopsis species of *Aegilops* and the origin of polyploid wheat B-subgenome. Mol. Plant **15**:488–503.

Li, M., Dong, L., Li, B., Wang, Z., Xie, J., Qiu, D., Li, Y., Shi, W., Yang, L., Wu, Q., et al. (2020). A CNL protein in wild emmer wheat confers powdery mildew resistance. New Phytol. **228**:1027–1037.

Ling, H.Q., Ma, B., Shi, X., Liu, H., Dong, L., Sun, H., Cao, Y., Gao, Q., Zheng, S., Li, Y., et al. (2018). Genome sequence of the progenitor of wheat A subgenome *Triticum urartu*. Nature **557**:424–428.

Liu, L., Zhang, Y., Tang, S., Zhao, Q., Zhang, Z., Zhang, H., Dong, L., Guo, H., and Xie, Q. (2010). An efficient system to detect protein ubiquitination by agroinfiltration in *Nicotiana benthamiana*. Plant J. **61**:893–903.

Liu, Y.G., and Huang, N. (1998). Efficient amplification of insert end sequences from bacterial artificial chromosome clones by thermal asymmetric interlaced PCR. Plant Mol. Biol. Rep. **16**:175–181.

Lu, P., Guo, L., Wang, Z., Li, B., Li, J., Li, Y., Qiu, D., Shi, W., Yang, L., Wang, N., et al. (2020). A rare gain of function mutation in a wheat tandem kinase confers resistance to powdery mildew. Nat. Commun. **11**:680.

Luo, M.C., Gu, Y.Q., Puiu, D., Wang, H., Twardziok, S.O., Deal, K.R., Huo, N., Zhu, T., Wang, L., Wang, Y., et al. (2017). Genome sequence of the progenitor of the wheat D genome *Aegilops tauschii*. Nature **551**:498–502.

Maccaferri, M., Harris, N.S., Twardziok, S.O., Pasam, R.K., Gundlach, H., Spannagl, M., Ormanbekova, D., Lux, T., Prade, V.M., Milner, S.G., et al. (2019). Durum wheat genome highlights past domestication signatures and future improvement targets. Nat. Genet. **51**:885–895.

McIntosh, R.A., Dubcovsky, J., Rogers, W.J., Morris, C., and Xia, X.C. (2017). Catalogue of Gene Symbols for Wheat: 2017 Supplement (KOMUGI Wheat Genetic Resource Database). https://shigen.nig.ac.jp/wheat/komugi/genes/symbolClassList.jsp.

Miller, T.E., Reader, S.M., Ainsworth, C.C., and Summer, R.W. (1988). The introduction of a major gene for resistance to powdery mildew of wheat, *Erysiphe graminis* f. sp. *tritici*, from *Aegilops speltoides* into wheat, *Triticum aestivum*. In Cereal Breeding Related to Integrated Cereal Production: Proceedings of the EUCARPIA Conference, M. Jorna and L. Shootmaker, eds. (Wageningen, Netherlands: Pudoc), pp. 179–183.

Moffett, P., Farnham, G., Peart, J., and Baulcombe, D.C. (2002). Interaction between domains of a plant NBS–LRR protein in disease resistance-related cell death. EMBO J. **21**:4511–4519.

Moore, J.W., Herrera-Foessel, S., Lan, C., Schnippenkoetter, W., Ayliffe, M., Huerta-Espino, J., Lillemo, M., Viccars, L., Milne, R., Periyannan, S., et al. (2015). A recently evolved hexose transporter variant confers resistance to multiple pathogens in wheat. Nat. Genet. **47**:1494–1498.

Müller, M.C., Kunz, L., Schudel, S., Lawson, A.W., Kammerecker, S., Isaksson, J., Wyler, M., Graf, J., Sotiropoulos, A.G., Praz, C.R., et al. (2022). Ancient variation of the *AvrPm17* gene in powdery mildew limits the effectiveness of the introgressed rye *Pm17* resistance gene in wheat. Proc. Natl. Acad. Sci. USA **119**. e2108808119.

Niewoehner, A.S., and Leath, S. (1998). Virulence of *Blumeria graminis* f. sp. *tritici* on winter wheat in the eastern United States. Plant Dis. **82**:64–68.

Praz, C.R., Bourras, S., Zeng, F., Sánchez-Martín, J., Menardo, F., Xue, M., Yang, L., Roffler, S., Böni, R., Herren, G., et al. (2016). *AvrPm2* encodes an RNase-like avirulence effector which is conserved in the two different specialized forms of wheat and rye powdery mildew fungus. New Phytol. **213**:1301–1314.

Qi, L.L., Wang, S.L., Chen, P.D., Liu, D.J., and Gill, B.S. (1998). Identification and physical mapping of three *Haynaldia villosa* chromosome-6V deletion lines. Theor. Appl. Genet. **97**:1042–1046.

Qi, X., Cui, F., Yu, L., Ding, A., Li, J., Chen, G., and Wang, H. (2010). Molecular tagging wheat powdery mildew resistance gene *Pm21* by EST-SSR and STS markers. Mol. Plant Breed. **8**:1–6.

Rairdan, G.J., Collier, S.M., Sacco, M.A., Baldwin, T.T., Boettrich, T., and Moffett, P. (2008). The coiled-coil and nucleotide binding domains of the potato Rx disease resistance protein function in pathogen recognition and signaling. Plant Cell **20**:739–751.

Sánchez-Martín, J., and Keller, B. (2019). Contribution of recent technological advances to future resistance breeding. Theor. Appl. Genet. **132**:713–732.

Sánchez-Martín, J., Steuernagel, B., Ghosh, S., Herren, G., Hurni, S., Adamski, N., Vrána, J., Kubaláková, M., Krattinger, S.G., Wicker, T., et al. (2016). Rapid gene isolation in barley and wheat by mutant chromosome sequencing. Genome Biol. **17**:221.

Sánchez-Martín, J., Widrig, V., Herren, G., Wicker, T., Zbinden, H., Gronnier, J., Spörri, L., Praz, C.R., Heuberger, M., Kolodziej, M.C., et al. (2021). Wheat *Pm4* resistance to powdery mildew is controlled by alternative splice variants encoding chimeric proteins. Nat. Plants **7**:327–341.

Sato, K., Abe, F., Mascher, M., Haberer, G., Gundlach, H., Spannagl, M., Shirasawa, K., and Isobe, S. (2021). Chromosome-scale

genome assembly of the transformation-amenable common wheat cultivar 'Fielder. DNA Res. **28**:dsab008.

Shen, Q.H., Saijo, Y., Mauch, S., Biskup, C., Bieri, S., Keller, B., Seki, H., Ulker, B., Somssich, I.E., and Schulze-Lefert, P. (2007). Nuclear activity of MLA immune receptors links isolate-specific and basal disease-resistance responses. Science **315**:1098–1103.

Singh, S.P., Hurni, S., Ruinelli, M., Brunner, S., Sanchez-Martin, J., Krukowski, P., Peditto, D., Buchmann, G., Zbinden, H., and Keller, B. (2018). Evolutionary divergence of the rye *Pm17* and *Pm8* resistance genes reveals ancient diversity. Plant Mol. Biol. **98**:249–260.

Song, W., Xie, C., Du, J., Xie, H., Liu, Q., Ni, Z., Yang, T., Sun, Q.,, and Liu, Z. (2009). A "one-marker-for-two-genes" approach for efficient molecular discrimination of *Pm12* and *Pm21* conferring resistance to powdery mildew in wheat. Mol. Breeding **23**:357–363.

Song, W., Xie, H., Liu, Q., Xie, C., Ni, Z., Yang, T., Sun, Q., and Liu, Z. (2007). Molecular identification of *Pm12*-carrying introgression lines in wheat using genomic and EST-SRR markers. Euphytica **158**:95–102.

Thompson, J.D., Higgins, D.G., and Gibson, T.J. (1994). Clustal W: improving the sensitivity of progressive multiple sequence alignment through sequence weighting position specific gap penalties and weight matrix choice. Nucleic Acids Res. **22**:4673–4680.

Walkowiak, S., Gao, L., Monat, C., Haberer, G., Kassa, M.T., Brinton, J., Ramirez-Gonzalez, R.H., Kolodziej, M.C., Delorean, E., Thambugala, D., et al. (2020). Multiple wheat genomes reveal global variation in modern breeding. Nature **588**:277–283.

Wan, Q., Wang, T., Ma, Y., Liu, W., Cao, Z., Qi, Y., Zhang, C., Ding, K., Fan, J., Zhou, Y., et al. (2021). Monitoring and analysis of virulence of *Blumeria graminis* f.sp. *tritici* population in Anhui Province. Acta Phytopathol. Sin. **51**:741–747. (In Chinese).

Wang, G.F., Ji, J., El-Kasmi, F., Dangl, J.L., Johal, G., and Balint-Kurti, P.J. (2015). Molecular and functional analyses of a maize autoactive NB-LRR protein identify precise structural requirements for activity. PLoS Pathog. **11**:e1004674.

Wang, J., Hu, M., Wang, J., Qi, J., Han, Z., Wang, G., Qi, Y., Wang, H.W., Zhou, J.M., and Chai, J. (2019a). Reconstitution and structure of a plant NLR resistosome conferring immunity. Science **364**:eaav5870.

Wang, J., Wang, J., Hu, M., Wu, S., Qi, J., Wang, G., Han, Z., Qi, Y., Gao, N., Wang, H.W., et al. (2019b). Ligand-triggered allosteric ADP release primes a plant NLR complex. Science **364**:eaav5868.

Wulff, B.B.H., and Moscou, M.J. (2014). Strategies for transferring resistance into wheat: from wide crosses to GM cassettes. Front. Plant Sci. **5**:692.

Wulff, B.B.H., Heese, A., Tomlinson-Buhot, L., Jones, D.A., de la Peña, M., and Jones, J.D.G. (2009). The major specificity-determining amino acids of the tomato Cf-9 disease resistance protein are at hypervariable solvent-exposed positions in the central leucine-rich repeats. Mol. Plant Microbe Interact. **22**:1203–1213.

Xie, J., Guo, G., Wang, Y., Hu, T., Wang, L., Li, J., Qiu, D., Li, Y., Wu, Q., Lu, P., et al. (2020). A rare single nucleotide variant in Pm5e confers powdery mildew resistance in common wheat. New Phytol. **228**:1011–1026.

Xing, L., Hu, P., Liu, J., Witek, K., Zhou, S., Xu, J., Zhou, W., Gao, L., Huang, Z., Zhang, R., et al. (2018). *Pm21* from *Haynaldia villosa* encodes a CC-NBS-LRR protein conferring powdery mildew resistance in wheat. Mol. Plant **11**:874–878.

Yahiaoui, N., Srichumpa, P., Dudler, R., and Keller, B. (2004). Genome analysis at different ploidy levels allows cloning of the powdery mildew resistance gene *Pm3b* from hexaploid wheat. Plant J. **37**:528–538.

Zhang, D., Zhu, K., Dong, L., Liang, Y., Li, G., Fang, T., Guo, G., Wu, Q., Xie, J., Chen, Y., et al. (2019). Wheat powdery mildew resistance gene *Pm64* derived from wild emmer (*Triticum turgidum* var. *dicoccoides*) is tightly linked in repulsion with stripe rust resistance gene *Yr5*. Crop J. **7**:761–770.

Zhang, J., Jiang, Y., Guo, Y., Li, G., Yang, Z., Xu, D., and Xuan, P. (2015). Identification of novel chromosomal aberrations induced by ^{60}Co-γ-irradiation in wheat-*Dasypyrum villosum* lines. Int. J. Mol. Sci. **16**:29787–29796.

Zhang, S., Zhang, R., Song, G., Gao, J., Li, W., Han, X., Chen, M., Li, Y., and Li, G. (2018). Targeted mutagenesis using the *Agrobacterium tumefaciens*-mediated CRISPR-Cas9 system in common wheat. BMC Plant Biol. **18**:302.

Zhao, G., Zou, C., Li, K., Wang, K., Li, T., Gao, L., Zhang, X., Wang, H., Yang, Z., Liu, X., et al. (2017). The *Aegilops tauschii* genome reveals multiple impacts of transposons. Nat. Plants **3**:946–955.

Zhao, Y.B., Liu, M.X., Chen, T.T., Ma, X., Li, Z.K., Zheng, Z., Zheng, S.R., Chen, L., Li, Y.Z., Tang, L.R., et al. (2022). Pathogen effector AvrSr35 triggers Sr35 resistosome assembly via a direct recognition mechanism. Sci. Adv. **8**:eabq5108.

Zhu, S., Ji, Y., Ji, J., Bie, T., Gao, A., and He, H. (2018). Fine physical bin mapping of the powdery mildew resistance gene *Pm21* based on chromosomal structural variations in wheat. Int. J. Mol. Sci. **19**:643.

Zou, S., Wang, H., Li, Y., Kong, Z., and Tang, D. (2018). The NB-LRR gene *Pm60* confers powdery mildew resistance in wheat. New Phytol. **218**:298–309.